Electronic Supplementary Material (ESI) for Journal of Materials Chemistry A.
This journal is © The Royal Society of Chemistry 2023

Supplementary Information

Unveiling the Multifunctional Regulation Effect of Glutamine for Highly-Reversible Zn Metal Anodes

Junyi Yin[a], Mingyan Li[a,b], Xiang Feng[a], Tianyi Cui[c], Jingzhe Chen[a], Fuxiang Li[a], Minghui Wang[a], Yonghong Cheng[a], Shujiang Ding[b], Xin Xu[a]*, and Jianhua Wang[a]*

[a] State Key Laboratory of Electrical Insulation and Power Equipment, School of Electrical Engineering, Xi'an Jiaotong University, Xi'an 710049, China

[b] Engineering Research Center of Energy Storage Materials and Devices, Ministry of Education and Xi'an Key Laboratory of Sustainable Energy Materials Chemistry, School of Chemistry, Xi'an Jiaotong University, Xi'an 710049, China

[c] China Power Complete Equipment Co., Ltd., Beijing 100080, China

*Corresponding authors.

E-mail addresses: xu.xin@xjtu.edu.cn (X. Xu); jhwang@mail.xjtu.edu.cn (J. Wang).

Density-Functional Theory Calculation Methods

All the computations were implemented with spin-polarized density functional theory (DFT) method, as performed by the Vienna ab initio simulation package (VASP)[1]. The projector augmented wavefunction (PAW) pseudo-potentials are used to describe ionic potentials[1]. The exchange correlation energy is sculptured by Perdew–Burke–Ernzerhof (PBE) functional within the generalized gradient approximation (GGA)[2]. In the course of the geometry relaxation, the energy cut-off was chosen as 500 eV. In structural optimizations, the Brillouin zone are sampled by 15 × 15 × 7 and 3 × 3 × 1 mesh points in k-space based on Monkhorst-Pack scheme[3] for Zn bulk and Zn(002) surface, respectively. The convergence criterion for the iteration in self-consistent field (SCF) is set to be 10^{-5} eV, and the force convergence criterion for atomic relaxation is set to be 0.02 eV /Å. Grimme's DFT-D3 methodology was used to describe the dispersion interactions. During structural optimizations, the bottom 2 atomic layers were fixed while the top two were allowed to relax for Zn (002). The vacuum gap is set as 15 Å to preclude interplay between two adjacent surfaces. The adsorption energy (ΔE_{ad}) of Glutamine and H_2O molecule on Zn (002) surface is defined as:

$$\Delta E_{ads} = E_{total} - E_{slab} - E_{molecule} \quad (1)$$

where E_{total} represents the total energy of the Glutamine or H_2O molecule adsorbed Zn (002) surface. E_{slab} represents the total energy of pure Zn (002) surface, $E_{molecule}$ is the total energy of H_2O or Glutamine molecule.

Experimental Section

Preparation of the Electrolytes.

To prepare 2 M $ZnSO_4$ electrolyte, $ZnSO_4 \cdot 7H_2O$ (Meryer, ≥99.5%) was dissolved into the deionized (DI) water. Then different amount of Gln powder was added to the 2 M $ZnSO_4$ electrolyte to obtain 0.1 M, 0.3 M and 0.5 M Gln-added electrolytes,

respectively. The optimized Gln concentration discussed in this paper is 0.3 M and marked as 'With Gln', unless otherwise stated.

Preparation of the Electrodes.

$NH_4V_4O_{10}$ cathode materials were prepared by a hydrothermal method[4]. Concretly, 0.585 g of ammonium vanadate (NH_4VO_3, Aladdin, 99%) was added into 35 mL DI water. After that, 0.9455 g oxalic acid ($H_2C_2O_4 \cdot 2H_2O$, Meryer, 99%) powders were added into the NH_4VO_3 solution under magnetically stirring. Then the solution was transferred to a 50 mL Teflon-lined autoclave and heated at 140 °C for 12 h. The products were collected and washed with DI water, then dried at 70 °C overnight to finally obtain the $NH_4V_4O_{10}$ powders. The cathode slurry was composed of 70% as-prepared active material, 20% super P (Timcal) and 10% polymer binder (PVDF, Macklin). The cathode was prepared by coating the slurry on the stainless foil and was dried at 80 °C under vacuum for 12 h. The mass loading of the active materials is around 1.0-2.0 mg cm^{-2}. The anode was served by Zn foil only.

Materials Characterization

Scanning electron microscope (SEM; ZEISS, Gemini 500) was used to acquire the morphology of anodes and cathodes with elemental mapping images. X-ray diffraction (XRD; Bruker D8 Advance) patterns of cathodes materials were recorded with a Cu Kα radiation (λ=1.54184 Å). Fourier transform infrared spectrometer (FTIR; Bruker VERTEX70) spectra of Zn anodes were obtained to analyze the adsorption of Gln on anodes. Raman (Renishaw Raman RE01) spectra were collected with a 633 nm laser.

Nuclear magnetic resonance (NMR; JNM-ECZ400S/L1) was employed to analyze the solvation structures of Zn^{2+} in electrolytes.

Electrochemical Measurements

The Zn symmetric cells and full cells for electrochemical tests were fabricated by assembling coin cells in air, employing glass microfiber (Whatman) as the separator, 80 μl of electrolytes were added to each cell. The electrolyte for Zn//$NH_4V_4O_{10}$ full cells was 2 M $ZnSO_4$ with/without 0.3 M Gln addictive. The electrochemical performance of the batteries was conducted on the Neware battery tester and an electrochemical workstation (CHI 760E, CH Instruments, Ins).

Supplementary Tables and Figures:

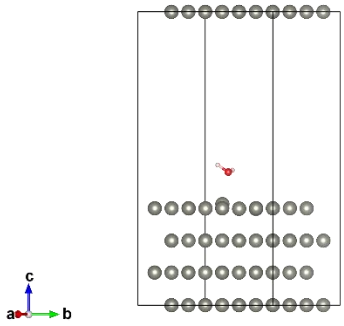

Figure S1 Calculation models of free H_2O molecule absorbed on Zn (002) plane.

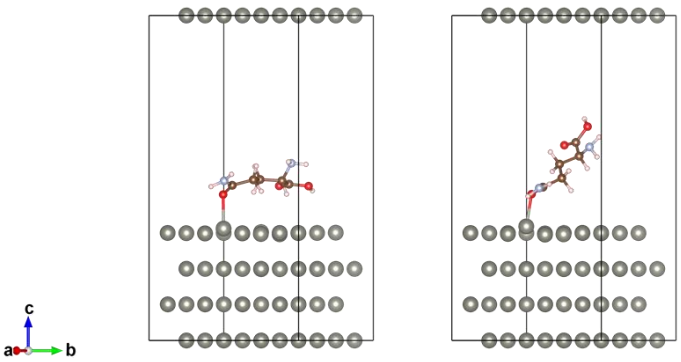

Figure S2 Calculation models of latericumbent (left) and recumbent (right) Gln molecule absorbed on Zn (002) plane.

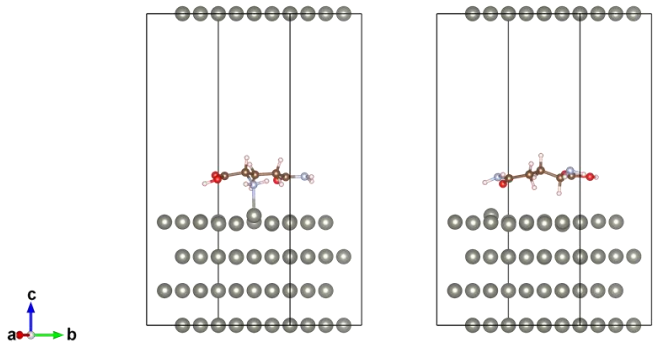

Figure S3 Calculation models of parallel Gln molecule absorbed on Zn (002) plane.

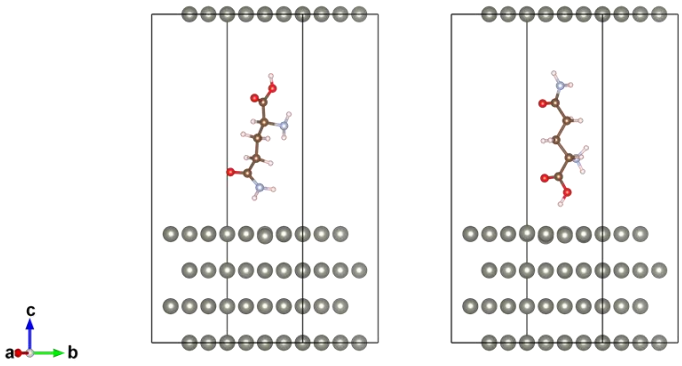

Figure S4 Calculation models of verticle Gln molecule absorbed on Zn (002) plane.

Table S1 Calculation results of H_2O and Gln molecule absorbed on Zn (002) plane.

Adsorbate	Total energy/eV	Base energy/eV	Molecular energy/eV	E_{abs}/eV
H_2O	-109.52377	-95.01767	-14.219016	-0.29
rec. gln	-218.19817	-95.01767	-119.75286	-3.43
lat. gln	-215.53253	-95.01767	-119.75286	-0.76
pall. gln 1	-216.15324	-95.01767	-119.75286	-1.38
pall. gln 2	-215.88195	-95.01767	-119.75286	-1.11
ver. gln 1	-215.19796	-95.01767	-119.75286	-0.43
ver. gln 2	-215.21414	-95.01767	-119.75286	-0.44

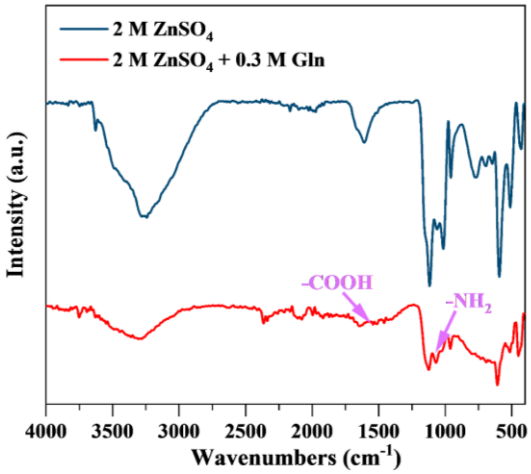

Figure S5 FTIR results of Zn anodes immersed in 2 M $ZnSO_4$ and 2 M $ZnSO_4$ + 0.3 M Gln electrolytes.

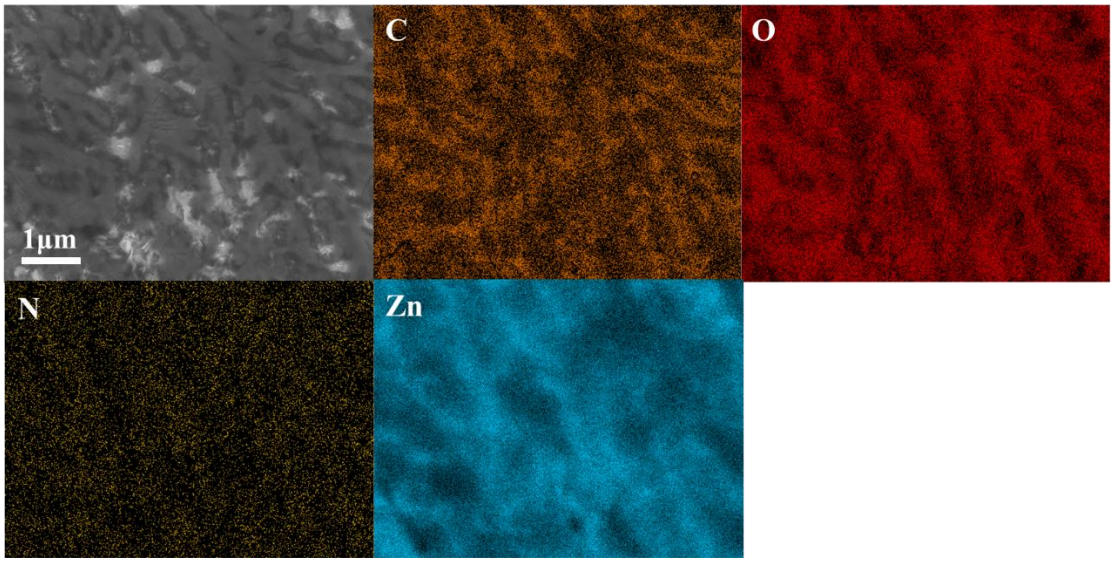

Figure S6 Morphology and corresponding element mapping of Zn anode with $ZnSO_4$/Gln electrolytes after cycling at 1 mA cm^{-2}, 1 mAh cm^{-2}.

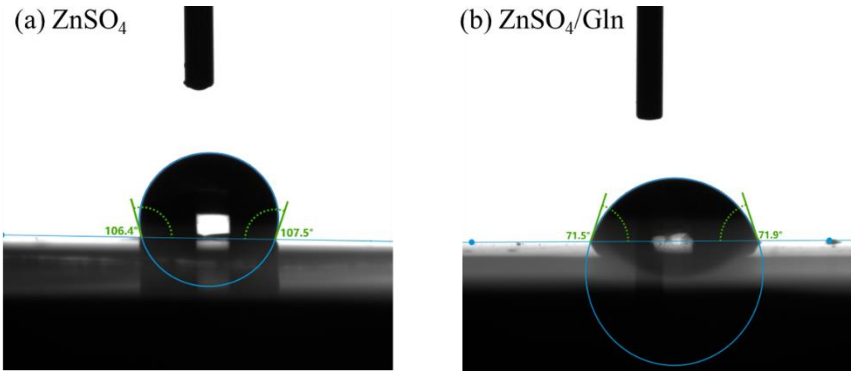

Figure S7 Contact angles of between $ZnSO_4$ electrolytes without (a) and with (b) Gln additive and Zn anode.

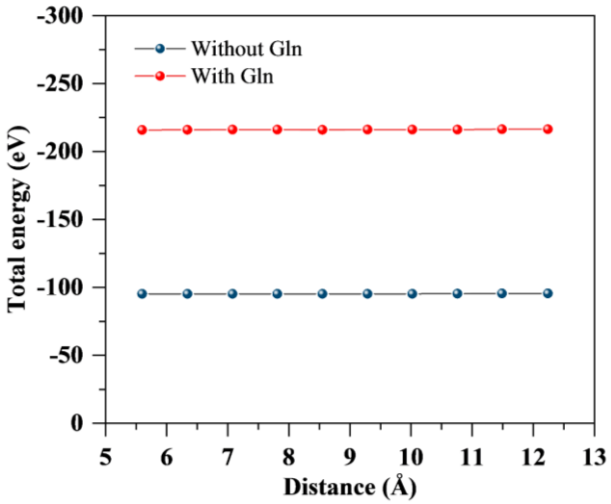

Figure S8 Calculation results of total energies of Zn^{2+} moving at different sites with and without Gln molecule absorbed on Zn (002) plane.

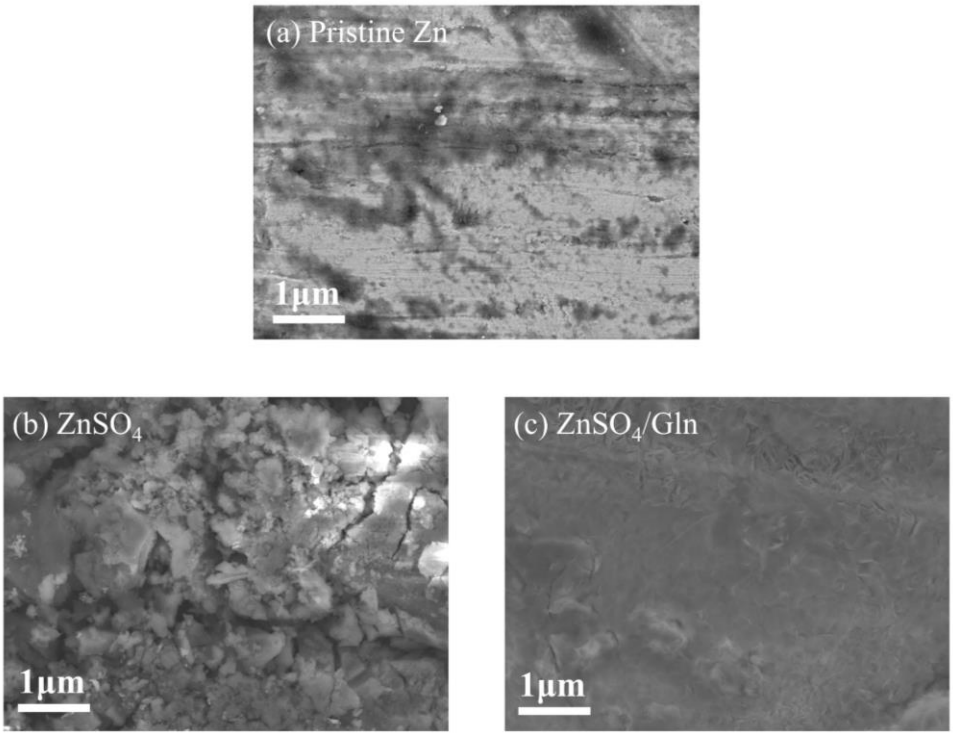

Figure S9 SEM images of pristine Zn (a) and Zn anodes cycled in $ZnSO_4$ electrolytes without (b) and with (c) Gln additive.

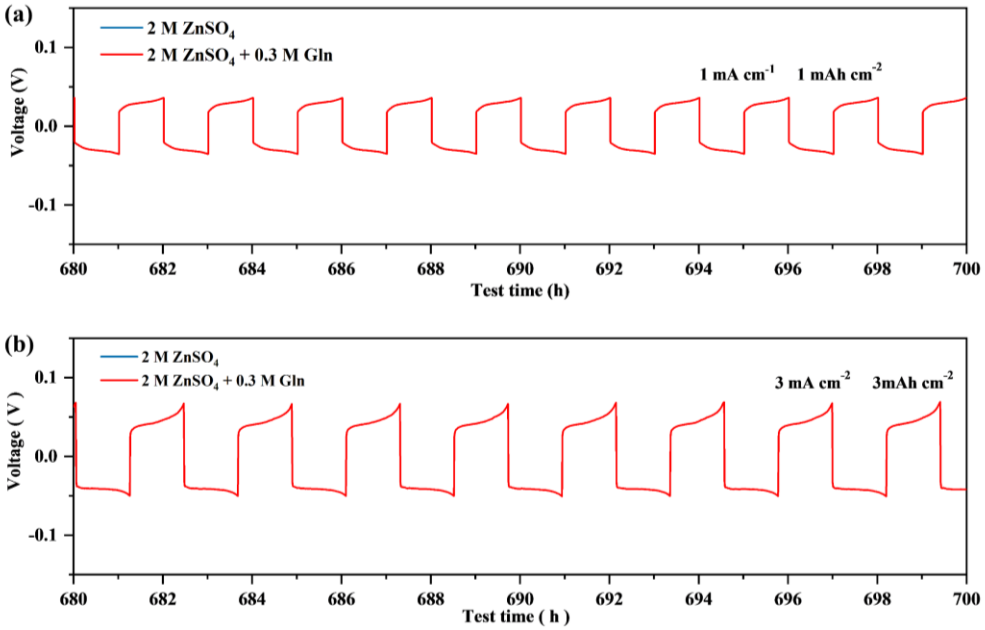

Figure S10 Cycling stability of Zn//Zn batteries with $ZnSO_4$ and $ZnSO_4$/Gln electrolytes under 1 mA cm^{-2} (a) and 1 mA cm^{-2} (b).

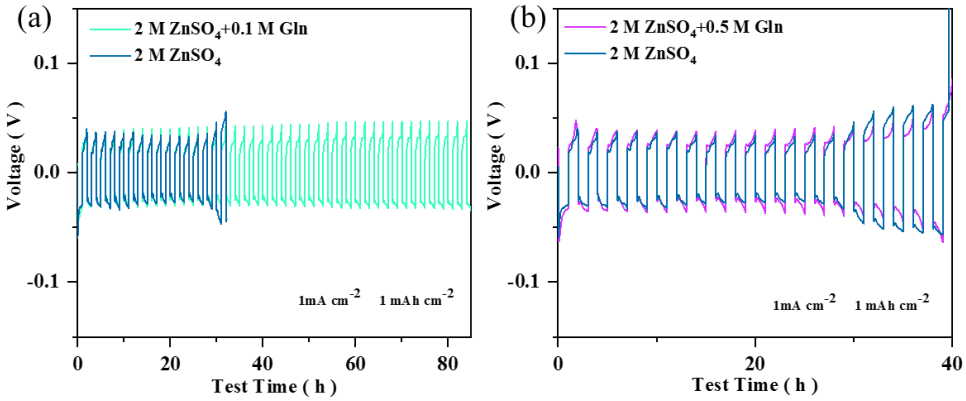

Figure S11 Cycling performance of Zn//Zn batteries in 2 M $ZnSO_4$ + 0.1 M Gln (a) and 2 M $ZnSO_4$ + 0.5 M Gln (b) electrolytes.

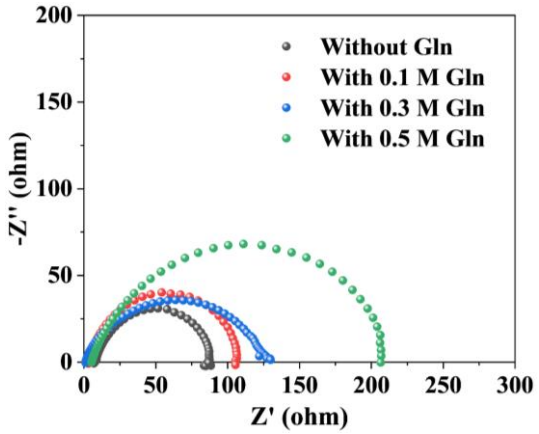

Figure S12 Electrochemical impedance spectroscopy of batteries assembled with Gln at different concentrations.

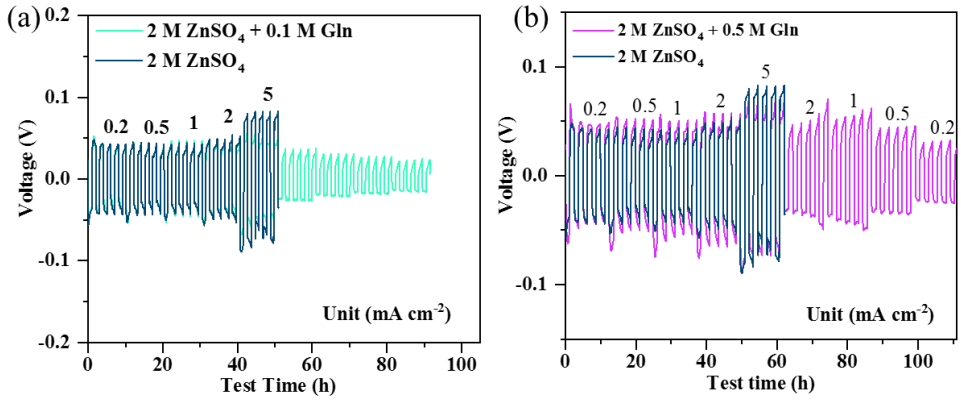

Figure S13 Rate performance of Zn//Zn batteries in 2 M $ZnSO_4$ + 0.1 M Gln (a) and 2 M $ZnSO_4$ + 0.5 M Gln (b) electrolytes.

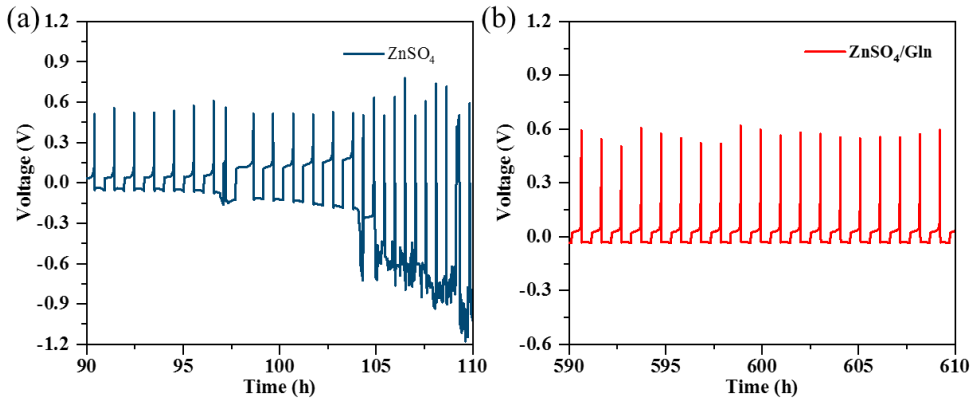

Figure S14 Performance of Zn//Cu batteries in 2 M $ZnSO_4$ (a) and 2 M $ZnSO_4$ + 0.3 M Gln (b) electrolytes.

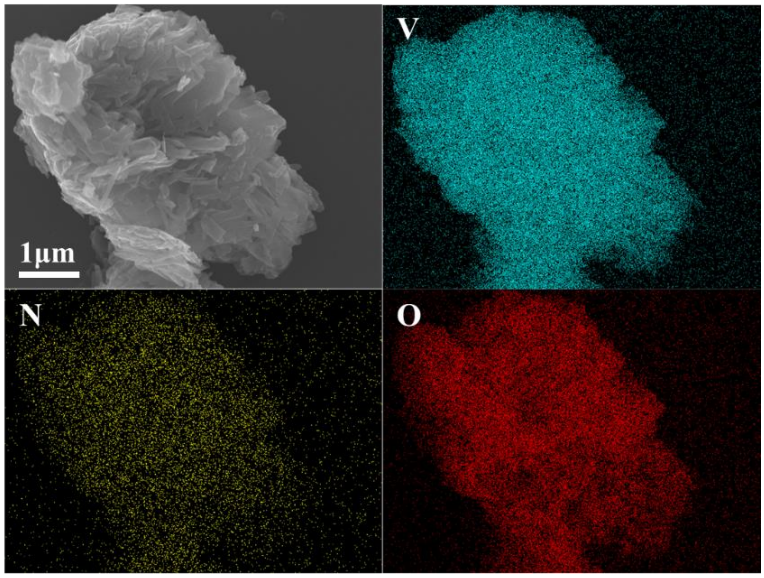

Figure S15 SEM images of $NH_4V_4O_{10}$ powder and corresponding element mappings.

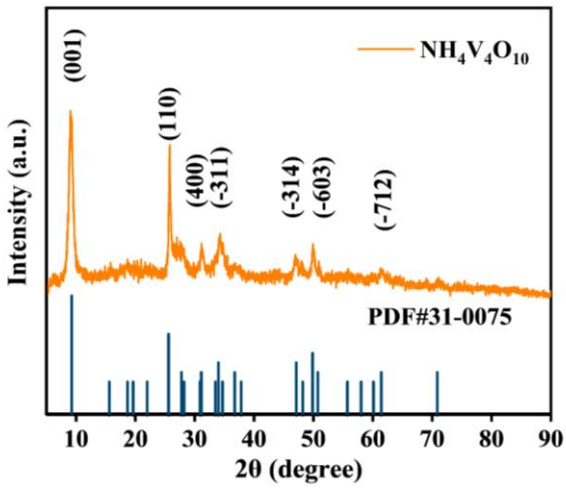

Figure S16 XRD patterns of $NH_4V_4O_{10}$ powder.

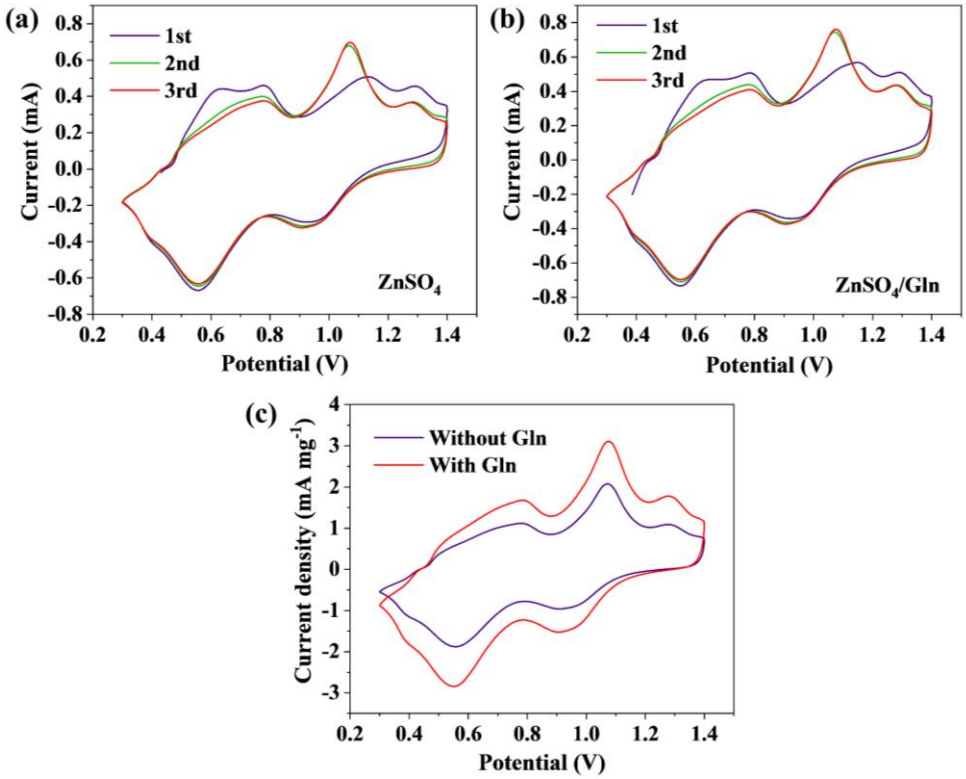

Figure S17 CV profiles of Zn//$NH_4V_4O_{10}$ batteries with different electrolytes. (a) pure $ZnSO_4$ and (b) 0.3 M $ZnSO_4$/Gln electrolyte. (c) Comparison of the 5^{th} cycle of CV curves.

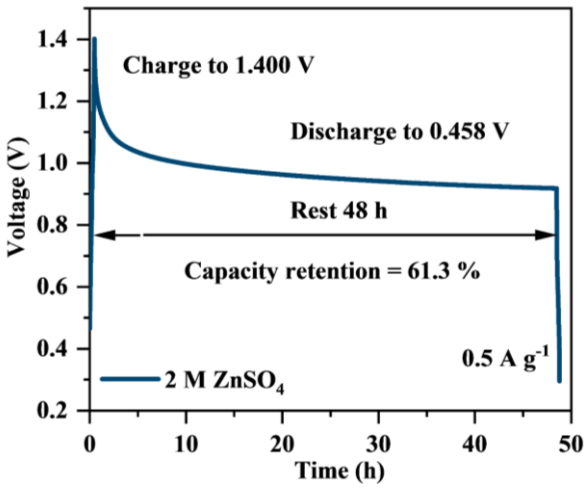

Figure S18 Capacity retention capability of Zn//$NH_4V_4O_{10}$ full batteries with pristine $ZnSO_4$ electrolyte

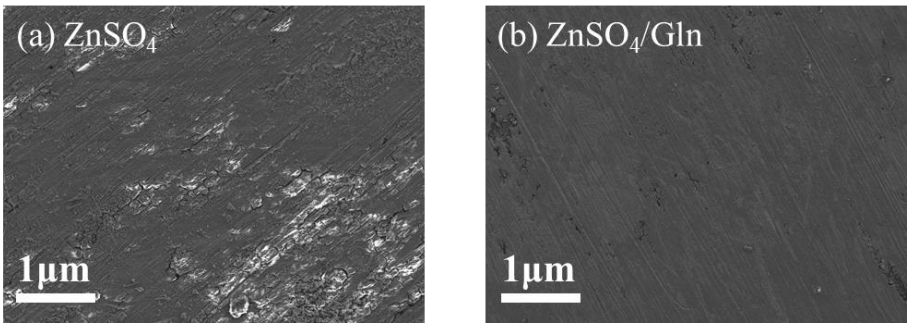

Figure S19 SEM images of Zn anodes in Zn//$NH_4V_4O_{10}$ full batteries. $ZnSO_4$ (a) and $ZnSO_4$/Gln (b).

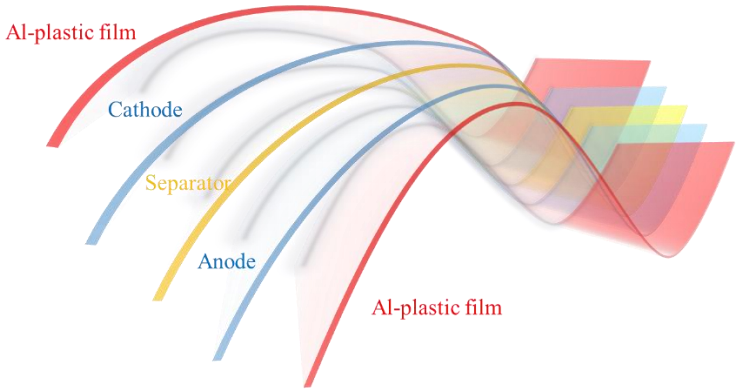

Figure S20 Structure illustration of flexible quasi-solid-state batteries.

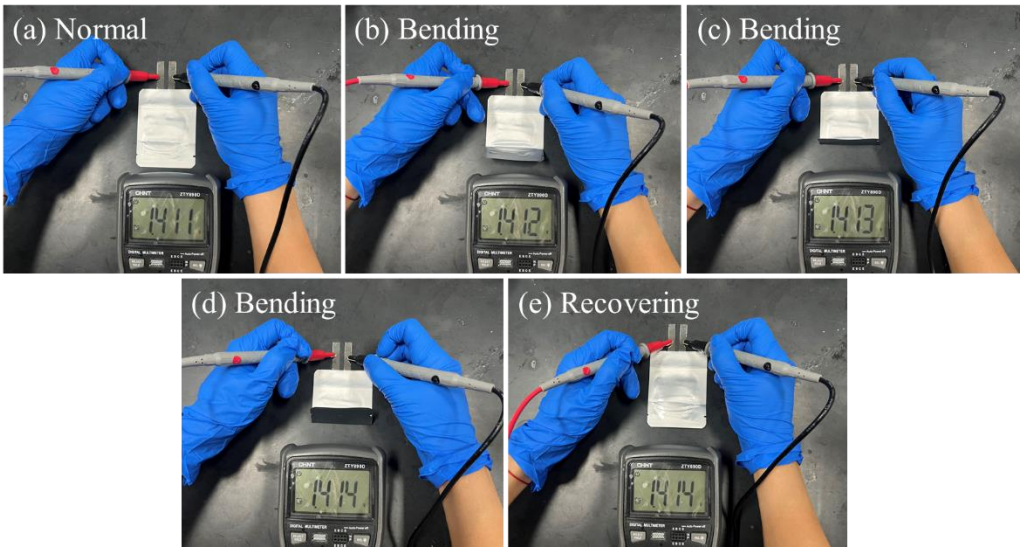

Figure S21 Optical photos of flexible pouch batteries with various degrees of bending. (a) Normal, (b-d) Bending, (e) Recovering.

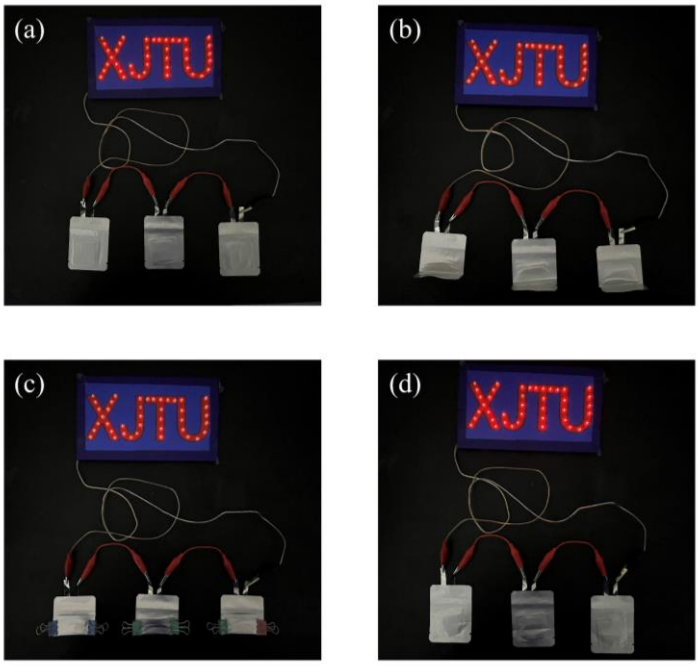

Figure S22 Application of flexible pouch batteries under different bending conditions. (a) Normal, (b) Bending 90°, (c) Bending 180°, (d) Recovering.

Table S2. Performance comparison of symmetric Zn//Zn cells from the previously reported works involving electrolyte additives and our work.

Electrolytes	**Current density/Areal capacity (mA cm^{-2}/mAh cm^{-2})**	**Lifespan (h)**	**CPC (Ah cm^{-2})**	**Refs.**
1 M $ZnAc_2$+4 M NH_4I	1/0.5	600	0.6	[5]
3 M $ZnSO_4$+10 mM α-CD	5/5	200	0.5	[6]
	10/1	160	0.8	
$ZnSO_4$-H_2O-NMP	1/1	1500	0.75	[7]
	5/10	200	0.5	
1 M $Zn(ClO_4)_2$+β-CD	1/1	1000	0.5	[8]
	5/5	350	0.875	
2.5 m $Zn(OTf)_2$+0.04 wt% POV	0.5/0.25	1000	0.5	[9]
1:4 m Zn/Li-70:30 wt% PEG/H_2O	0.25/0.4	500	0.125	[10]
2 m $ZnSO_4$+0.0085 m $La(NO_3)_3$	1/1	1200	0.6	[11]
50%-Bet/$ZnSO_4$	0.5/0.5	4200	1.05	[12]
	2/2	830	0.83	
2 M $ZnSO_4$ in glycerol/water (50/50)	1/1	1500	0.9	[13]
	2/6	900		
2 M $ZnSO_4$+0.08 M ZnF_2	1/1	600	0.3	[14]
2 M $ZnSO_4$+5 mM vanilli	1/1	1000	0.5	[15]

1 M $ZnSO_4$+4 M EMImCl	1/1	500	0.25	[16]
1 M $ZnSO_4$+0.1 M TSC	5/1.25	200	0.5	[17]
1 M $Zn(CF_3SO_3)_2$+25 mM $Zn(H_2PO_4)_2$	1/1	1200	0.6	[18]
	1/5	800	0.4	
3 M $Zn(CF_3SO_3)_2$+20 mM $Zn(NO_3)_2$	0.5/0.5	1200	0.3	[19]
7.6 m $ZnCl_2$+0.05 m $SnCl_2$	3/3	500	0.75	[20]
2 M $ZnSO_4$+1 vol% DME	2/2	380	0.38	[21]
3 M $ZnSO_4$ in H2O/68 vol% EG	0.5/0.5	2268	0.667	[22]
1.3 m $ZnCl_2$ in H_2O/DMSO (4.3/1)	0.5/0.5	1000	0.25	[23]
4 M $Zn(BF_4)_2$+2 mM $Al(OTf)_3$	1/0.5	1900	0.9	[24]
2 M $ZnSO_4$+0.3 M Gln	3/3	700	1.05	This work

References

[1] G. Kresse, D. Joubert, *Phys. Rev. B.* **1999**, 59, 1758.

[2] J. P. Perdew, K. Burke, M. Ernzerhof, *Phys. Rev. Lett.* **1996**, 77, 3865.

[3] D. J. Chadi, *Phys. Rev. B.* **1977**, 16, 1746.

[4] B. Tang, J. Zhou, G. Fang, F. Liu, C. Zhu, C. Wang, A. Pan, S. Liang, *J. Mater. Chem. A* **2019**, **7**, 940.

[5] Q. Zhang, Y. L. Ma, Y. Lu, Y. X. Ni, L. Lin, Z. K. Hao, Z. H. Yan, Q. Zhao, J. Chen, *J. Am. Chem. Soc*. **2022**, 144, 18435.

[6] K. Zhao, G. L. Fan, J. D. Liu, F. M. Liu, J. H. Li, X. Z. Zhou, Y. X. Ni, M. Yu, Y. M. Zhang, H. Su, Q. H. Liu, F. Y. Cheng, *J. Am. Chem. Soc.* **2022**, 144, 11129.

[7] D. Wang, D. Lv, H. Liu, S. Zhang, C. Wang, C. Wang, J. Yang, Y. Qian, *Angew. Chem., Int. Ed.* **2022**, e202212839.

[8] M. J. Qiu, P. Sun, Y. Wang, L. Ma, C. Y. Zhi, W. J. Mai, *Angew. Chem., Int. Ed.* **2022**, 61, e202210979.

[9] K. Yang, Y. Y. Hu, T. S. Zhang, B. Y. Wang, J. X. Qin, N. X. Li, Z. W. Zhao, J. W. Zhao, D. L. Chao, *Adv. Energy Mater*. **2022**, 12, 2202671.

[10] D. E. Ciurduc, C. de la Cruz, N. Patil, A. Mavrandonakis, R. Marcilla, *Energy Storage Mater.* **2022**, 53, 532.

[11] R. R. Zhao, H. F. Wang, H. R. Du, Y. Yang, Z. H. Gao, L. Qie, Y. H. Huang, *Nat. Commun.* **2022**, 13, 3252.

[12] H. Ren, S. Li, B. Wang, Y. Zhang, T. Wang, Q. Lv, X. Zhang, L. Wang, X. Han, F. Jin, C. Bao, P. Yan, N. Zhang, D. Wang, T. Cheng, H. Liu, S. Dou, *Adv. Mater.* **2022**, e2208237.

[13] Y. J. Zhang, M. Zhu, K. Wu, F. F. Yu, G. Y. Wang, G. Xu, M. H. Wu, H. K. Liu, S. X. Dou, C. Wu, *J. Mater. Chem. A* **2021**, 9, 4253.

[14] Y. An, Y. Tian, K. Zhang, Y. Liu, C. Liu, S. Xiong, J. Feng, Y. Qian, *Adv. Funct. Mater.* **2021**, 31, 2101886.

[15] K. Zhao, F. Liu, G. Fan, J. Liu, M. Yu, Z. Yan, N. Zhang, F. Cheng, *ACS Appl. Mater. Interfaces* **2021**, 13, 47650.

[16] Q. Zhang, Y. Ma, Y. Lu, X. Zhou, L. Lin, L. Li, Z. Yan, Q. Zhao, K. Zhang, J. Chen, *Angew. Chem., Int. Ed.* **2021**, 60, 23357.

[17] N. Wang, S. Zhai, Y. Ma, X. Tan, K. Jiang, W. Zhong, W. Zhang, N. Chen, W. Chen, S. Li, G. Han, Z. Li, *Energy Storage Mater.* **2021**, 43, 585.

[18] X. Zeng, J. Mao, J. Hao, J. Liu, S. Liu, Z. Wang, Y. Wang, S. Zhang, T. Zheng, J. Liu, P. Rao, Z. Guo, *Adv. Mater.* **2021**, 33, e2007416.

[19] D. Li, L. Cao, T. Deng, S. Liu, C. Wang, *Angew. Chem., Int. Ed.* **2021**, 60, 13035.

[20] L. Cao, D. Li, F. A. Soto, V. Ponce, B. Zhang, L. Ma, T. Deng, J. M. Seminario, E. Hu, X. Q. Yang, P. B. Balbuena, C. Wang, *Angew. Chem., Int. Ed.* **2021**, 60, 18845.

[21] J. Cui, X. Liu, Y. Xie, K. Wu, Y. Wang, Y. Liu, J. Zhang, J. Yi, Y. Xia, *Mater. Today Energy* **2020**, 18, 100563.

[22] R. Qin, Y. Wang, M. Zhang, Y. Wang, S. Ding, A. Song, H. Yi, L. Yang, Y. Song, Y. Cui, J. Liu, Z. Wang, S. Li, Q. Zhao, F. Pan, *Nano Energy* **2021**, 80, 105478.

[23] L. Cao, D. Li, E. Hu, J. Xu, T. Deng, L. Ma, Y. Wang, X. Q. Yang, C. Wang, *J. Am. Chem. Soc.* **2020**, 142, 21404.

[24] L. Ma, S. Chen, X. Li, A. Chen, B. Dong, C. Zhi, *Angew. Chem., Int. Ed.* **2020**, 59, 23836.